

Investigations on the synthesis and growth and structural, spectral, optical, mechanical and thermal properties of non-linear optical single crystals of Bis-L-Seriniumoxalate Dihydrate (BLSOD)

A. M. Hidayathullah^{a,b}, R. S. Samuel^{a,c}, V. Chithambaram^{d,*}, R. Raja^{a,e}, S. Janarthanan^f,

^aCenter for research and evaluation, Bharathiar University, Coimbatore, Tamilnadu, India

^bDepartment of Physics, Aalim Muhammed Salegh College of Engineering, Avadi, Chennai, Tamil Nadu, India

^cDepartment of Physics, The New College, Royapettah, Chennai, Tamil Nadu, India

^dDepartment of Physics, Karpaga Vinayaga College of Engineering and Technology, Chengalpattu, Chennai, Tamilnadu, India

^eDepartment of Physics, S.A. Engineering College, Chennai, Tamil Nadu, India

^fDepartment of Physics, Adhi College of Engineering and Technology, Sankarapuram, Kanchipuram, Tamil Nadu, India

From the raw materials L-Serine and oxalic acid, the product Bis-L-Seriniumoxalatedehydrate(BLSOD) was created. By using a slow evaporation process, the individual BLSOD crystals were produced from aqueous solution. According to single crystal X-ray Diffraction investigations, the structure of the produced crystal is monoclinic. The existence of different functional groups and the chemical environment present in the synthesised material were qualitatively determined through the use of Fourier Transform Infra-Red (FTIR) and proton nuclear magnetic resonance (1H NMR) spectrum studies. The crystal's transparency in the visible and near-infra-red areas was confirmed by UV-Visible-Near infrared and photoluminescence spectrum tests, which also looked at the material's viability for device construction. To determine the crystal's machinability, the mechanical properties of the material were carefully examined using Vicker's hardness research. Thermal investigations such as Thermo gravimetric (TGA) and Differential thermal analysis (DTA) have shown the thermal stability of BLSOD and the phases of weight losses. As a function of frequency and temperature, the dielectric constant and dielectric loss of grown crystals were determined. The Kurtz-Perry powder test was used to check both the second harmonic generation (SHG) and then the NLO property of the material.

(Received September 21, 2022; Accepted January 10, 2023)

Keywords: Single crystal, Slow evaporation, TGA, DTA, SHG, NLO

1. Introduction

In recent days, nonlinear optical (NLO) materials have become the key elements in solid state laser and frequency conversion techniques that have important applications in many fields, such as advanced laser-based imaging, optical communication, and data storage systems [1]. In the field of crystal engineering, the evolution of single crystals with self-assembled hydrogen bonds in their molecular structure has received considerable attention [2]. The coherent blue and green light emitted by nonlinear optical materials is important for many applications like displays, high-resolution printing, and signal processing, etc. [3-5]. These NLO materials, in the form of their single crystals, are the basis of all contemporary technology [6-8]. Semi-organic materials have high optical linearity, are resistant to laser-induced damage, have an inherent ultra-fast response

* Corresponding author: chithambaramv@gmail.com
<https://doi.org/10.15251/JOR.2023.191.43>

time, have low angular sensitivity, and have good mechanical stability [9, 10]. Chemical purity and structural composition are evaluated together to determine an effective SHG sample's optical response [11]. Organic molecular materials with a high degree of delocalized electrons have received a great deal of attention due to the compound's additional supporting nonlinear response [12]. Amino acids are attractive materials in the field of nonlinear optics because they have higher SHG efficiency than conventional KDP [13, 14]. Thus, the curiosity of researchers is focused on amino acids, which have a group of hydrogen-bonded nature that show very good NLO properties [15, 16]. This NLO behaviour is attributed to the presence of a proton donor carboxyl acid (COOH) group and a proton acceptor (NH_2) group in amino acids. The molecular hyperpolarizability (β) is the basis of a strong SHG response. The zwitter ionic form of L-serine can be combined with anionic, cationic, and neutral constituents. It is one of the naturally occurring protein-genic amino acids. Recent studies have also revealed that many oxalates of the amino acid family which have directly linked two carboxyl groups also primarily show SHG behaviour [17]. Oxalic acid, commonly known as ethanedioic acid, is an organic acid with the formula $\text{C}_2\text{H}_2\text{O}_4$. It is the most basic dicarboxylic acid. It is a white crystalline solid that dissolves in water to create a colourless solution. It is found naturally in a variety of foods. In this paper we report on the synthesis and growth and structural, spectral, optical, mechanical, and thermal characterizations of BLSOD single crystals grown by the slow evaporation technique.

2. Experimental details

2.1. Synthesis and crystal growth of BLSOD

The starting materials, L-Serine and oxalic acid of high purity (AR grade), were procured from Sigma-Aldrich. L-serine is an α -amino acid that is polar, uncharged, and has a hydroxymethyl group on its side chain. Oxalic acid is an organic compound. The L-Serine and Oxalic acid were taken in a 2:1 stoichiometric ratio and dissolved in double distilled water to prepare the aqueous solution of BLSOD. The solution was continuously stirred and slightly heated above the room temperature to obtain a homogeneous mixture over the entire volume. The expected chemical reaction is given in Fig. 1. The prepared solution was filtered twice using Whatmann filter paper in order to eliminate suspended impurities. At room temperature, the purified solution was allowed to evaporate, which yielded the salt of Bis-L-Seriniumoxalatedihydrate (BLSOD). The substance was successively recrystallized using deionized water to ensure high purity. The transparent colourless crystals were harvested after a period of 45 days. Fig. 2 shows the grown crystals of BLSOD from its aqueous solution by a slow evaporation technique.

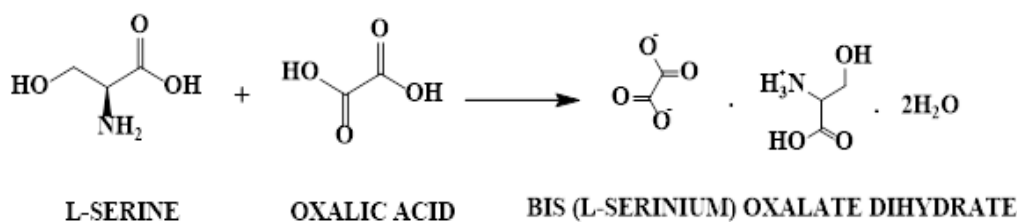


Fig. 1. Chemical reaction of BLSOD.

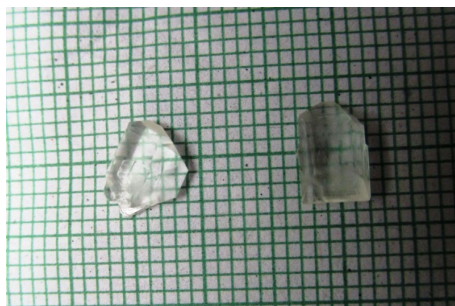


Fig. 2. The grown crystal of BLSOD

2.2. Characterization

A single crystal XRD study of the DLLM crystal was performed to obtain cell parameters using an ENRAF NONIUS CAD4 diffractometer and incident $\text{MoK}\alpha$ radiation of wavelength 0.71073 \AA . The powder XRD analysis of the sample was performed using a REICH SEIFERT X-ray diffractometer and incident $\text{CuK}\alpha$ radiation of wavelength 1.54058 \AA . Using a BRUKER IFS66V FTIR spectrophotometer, the functional groups in the sample were studied in the 400 cm^{-1} to 4000 cm^{-1} range. The sample's molecular structure was confirmed using a BRUKER 300 MHz spectrometer in DMSO solvent, with TMS as the internal reference standard. The optical transparency of the crystal was investigated using a PERKIN ELMER LAMBDA35 spectrophotometer in the wavelength range of 200 nm to 800 nm. The Lumina Fluorescence Spectrometer was used for the photoluminescence study. The LEITZ WETZLER Vickers micro hardness tester was used to assess mechanical strength. The dielectric nature of the crystal was studied using HIOKI 3532 LCR HITESTER in the frequency region of 50Hz–5MHz. The sample's thermal stability was determined using TG/DTA on a NETZSCH STA 449F5 thermal analyzer. The second-order nonlinearity was determined using the Kurtz and Perry powder technique.

3. Results and discussion

3.1. Single crystal XRD analysis

The compound's crystal structure, lattice parameters, and crystalline phases were calculated using single crystal and powder XRD analyses. XRD analysis is a nondestructive method for determining the crystal structure of compounds. It provides detailed information about the molecular structure, bond lengths, bond angles, unit cell parameters, and space groups. The lattice parameters were estimated to be $a = 5.11 \text{ \AA}$, $b = 12.57 \text{ \AA}$, $c = 11.08 \text{ \AA}$, $\alpha = \gamma = 90^\circ$ and $\beta = 99.85^\circ$ with $V = 701.20 (\text{ \AA})^3$. The crystal belongs to the monoclinic crystal system with space group P21 which agrees well with the available reported literature values [18].

The powder X-ray diffraction study was performed on the grown crystal powder form. The compound's diffraction peaks are proportional to the fraction of constituents in the compound. The comparison of the diffraction peak intensity of the mixture to the pure material's peak intensity does not provide the most reliable consideration. The powder XRD pattern of BLSOD is shown in Fig. 3. The sample of BLSOD was scanned at a rate of $3^\circ / \text{min}$ in the range from 10° to 80° . The peaks were indexed using TJB Holland & SAT Redfern unit cell software package. The plane (3 1 1) of BLSOD showed the highest intensity. All the peaks in the pattern were indexed as shown in Fig. 3. In powder XRD, the slight decline in the intensity of the peak might be due to the presence of the metal in the compound [19].

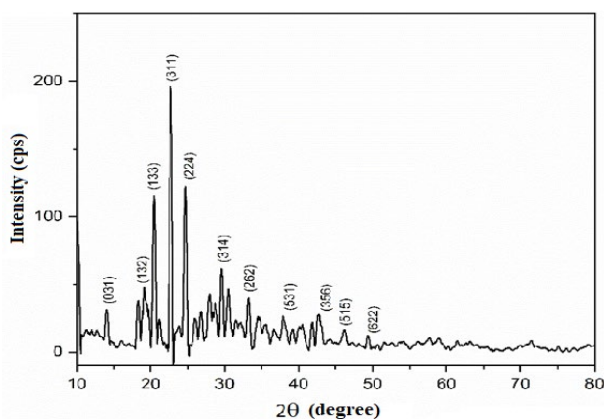


Fig. 3. Powder XRD of BLSOD.

3.2. FTIR spectral analysis

The emission or absorption spectrum from the FTIR spectrometer was investigated using FTIR spectroscopy over a wide range of wavenumber (4000 cm^{-1} to 400 cm^{-1}). The primary goal of this technique is to measure the amount of light absorbed by the sample during electromagnetic radiation interaction with the material [20]. The unique fingerprint of a molecule distinguishes one from another [21].

FTIR spectral analysis is a useful technique to identify the functional groups of the grown crystals. The FTIR spectrum of BLSOD is shown in Fig. 4. In this spectrum, signals at 3261 cm^{-1} and 3341 cm^{-1} are due to $-\text{OH}$ stretching vibrations of the carboxylic acid group of serine molecules [22]. The peak at 2973 cm^{-1} is due to the alkyl stretching vibration of the serine molecule. The small vibration at 2765 cm^{-1} is due to the presence of intermolecular hydrogen bonding between the two serine carboxylic acid groups. The peaks at 1382 cm^{-1} and 1087 cm^{-1} can be attributed to the NH stretching and bending vibration of the NH_2 group of amino acids. The strong vibrational peak at 1590 cm^{-1} may be due to the carboxyl group of carboxylic acids of oxalic acid and serine molecules. The FTIR spectral studies confirmed the presence of water of crystallization, oxalate, and serine groups in the grown crystals.

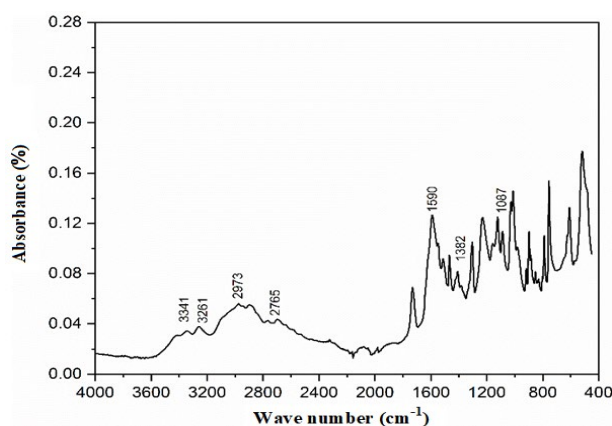


Fig. 4. FTIR spectrum of BLSOD

3.3. ^1H NMR spectral analysis

Nuclear magnetic resonance (NMR) spectroscopy is a key technique in the field of material science and engineering [23]. The NMR signal is produced by the nuclei of atoms with spin $1/2$ that are located in a magnetic field. The NMR spectrum determines the chemical groups in the molecule and provides structural information. "Chemical shift" is the frequency interval between resonance and the reference expressed in parts per million (ppm) [24].

The NMR technique is used to detect the presence of particular nuclei in a compound and also the position of carbon atoms for a given nuclear species. It is also an important tool for the identification of molecules and the examination of their electronic structures [25]. The ^1H NMR spectrum of BLSOD, shown in Fig. 5, has well resolved characteristic peaks for different types of chemical environments present in the compound. The sharp singlet at 3.62 ppm is due to the presence of an aliphatic hydrogen group in the compound. The appearance of two triplets at 4.56 ppm and 4.61 ppm are characteristics of the methylene ($-\text{CH}_2$) group and methine ($-\text{CH}$) group present in the compound, respectively. The down field value of ($-\text{CH}$), i.e., at 4.52 ppm, is due to the presence of an aliphatic ($-\text{COOH}$) group and quaternary ammonium attached to that carbon atom. The broad signal/singlet at 11.03 ppm corresponds to the aliphatic carboxylic acid group present in the compound. Interestingly, a singlet at 4.36 ppm is due to the presence of water hydration. The structural information derived using the ^1H NMR spectrum clearly conforms to the microstructure of the synthesized compound (BLSOD).

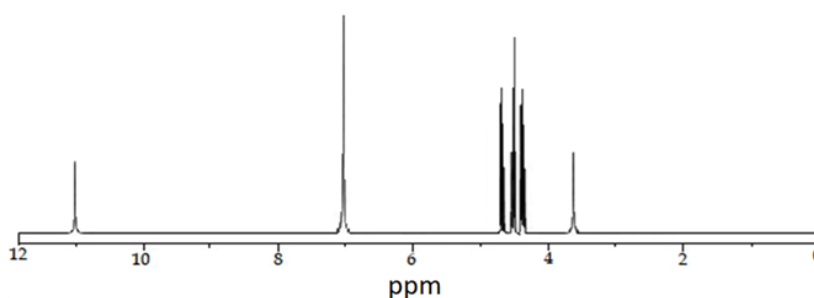


Fig. 5. ^1H NMR spectrum of BLSOD.

3.4. UV-Vis-NIR spectral analysis

An UV-Vis-NIR spectral study is useful to determine the transparency of a material, which is an important requirement for the material to be optically active [26]. A sample absorbed light of a wavelength in the UV region for the transition of an electron from a lower energy level to a higher energy level and was not absorbed in the visible and near-infrared regions of incident electromagnetic radiation [27]. The UV-Vis-NIR spectrum of BLSOD is shown in Fig. 6.

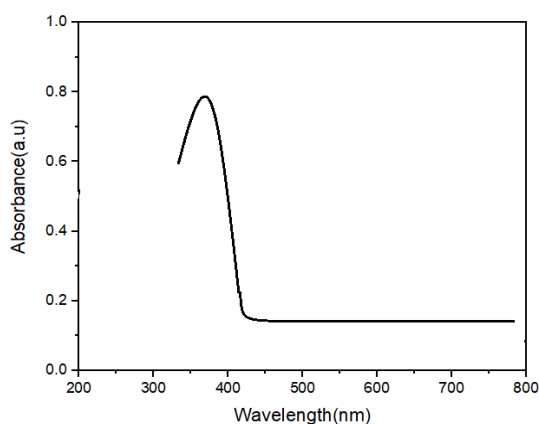


Fig. 6. UV-Vis-NIR spectrum of BLSOD

The spectrum has excellent transmission throughout the visible region. The wavelength of the lower cutoff was discovered to be 380 nm. For NLO applications, crystal transparency in the visible region is a desirable property. The band gap energy of the BLSOD was calculated using the relation, $E_g = 1240/\lambda$. The band gap is calculated to be 3.26 eV.

3.5. Photoluminescence study

The photoluminescence study analyses the emission of light due to photo excitations [28]. It is studied in the range from 400 to 700 nm with an excitation wavelength of 380 nm chosen from the UV-Vis-NIR spectrum [29]. The obtained spectrum is depicted in Fig. 7. The transmission of protons from carboxylic acid to amino group endorses the emission of green light at 540 nm in the photoluminescence spectrum. The luminescent nature of this material confirms its applicability in optical data storage devices [30].

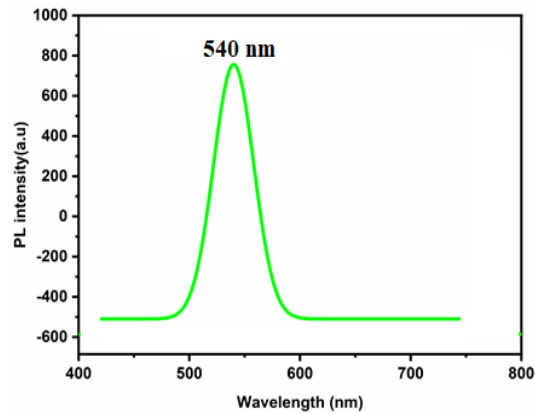


Fig. 7. Photoluminescence spectra of BLSOD.

3.6. Vicker's micro hardness test

The micro hardness test of the BLSOD material was carried out using a Leitzmicrohardness tester fitted with a diamond pyramidal indenter [31]. The mechanical stability of crystalline solids is closely related to the structure and composition of the material. Vickers hardness is the most important deciding factor in the fabrication of the device during various processes such as cutting and polishing of the crystal [1]. The strength of the crystalline solid is related to structure and bonding, which is essential for optoelectronic device fabrication [32]. The hardness indicates the resistance of the material to the local deformation triggered by indentation [33]. The applied load was changed from 10 g to 100 g for a period of about 10 s. A graph plotted between hardness number and the load (Fig. 8) shows an increase in hardness number with load up to 90 g and then a decrease with an increase in load. This indicates that this material is suitable for optoelectronic device fabrication. The hardness number is calculated using the formula,

$$H_V = 1.8544 P/d^2 \text{ (Kg /mm}^2\text{)} \quad (1)$$

where, H_V is the Vicker's hardness number, P is the load in kg, and d is the diagonal impression for the various loads.

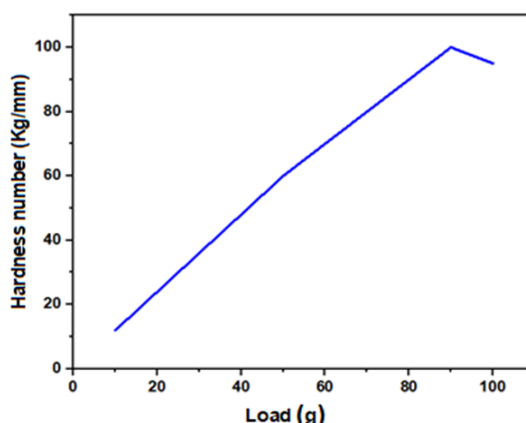


Fig. 8. Vickers micro hardness study of BLSOD.

3.7. Thermal analyses

Thermally stable NLO crystals are very much in demand for device fabrication. The TGA and DTA analyses give evidence of phase transition, melting point, and temperature-dependent mass change of a substance [34]. Thermogravimetric (TG) analysis measures the change in mass of a material as a function of temperature. In differential thermal analysis (DTA), the sample temperature is compared to the temperature of the reference material. It is always recommended to use both TG and DTA to understand mass change in relation to temperature [35]. The TGA trace of BLSOD, shown in Fig. 9 indicates that the material exhibits weight loss at a temperature of 183 °C due to decomposition of BLSOD compound. It was observed that the BLSOD is stable up to 183 °C. The DTA curve of BLSOD shows a very sharp exothermic peak at 182 °C which corresponds to the melting of BLSOD.

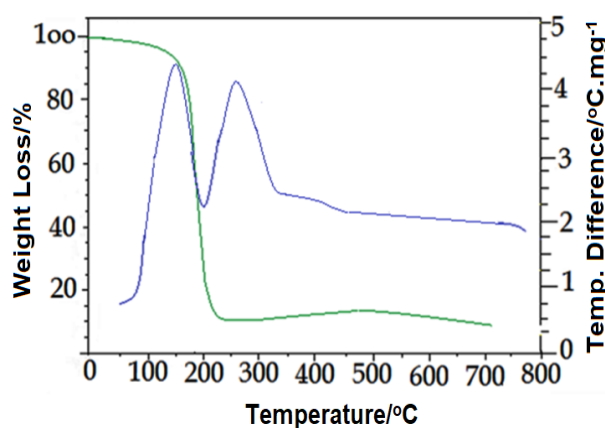


Fig. 9. TG-DTA trace of BLSOD.

3.8. Dielectric studies

Dielectric studies on BLSOD crystals were carried out at various frequencies. The dielectric constant (ϵ_r) and dielectric loss ($\tan \delta$) are affected by the frequency of the applied field. Fig. 10 depicts the variation of the dielectric constant with frequency. As the frequency increases, the value of the dielectric constant decreases. The high value of dielectric constant in the low frequency region may be due to contributions from all four polarizations. When the number of ions in the crystals changes electronically, local electrons move in the direction of the applied field. This is called polarization [36].

As the frequency increases, a point will be reached where the space charge cannot sustain and comply with the external varying field, causing the dielectric constant to decrease. Fig 11 shows that the continuous and gradual decrease in dielectric constant suggests that BLSOD

crystals, like any other normal dielectric, may have domains of varying sizes and relaxation times. The dielectric loss is a way to figure out how much energy the dielectric takes in [37].

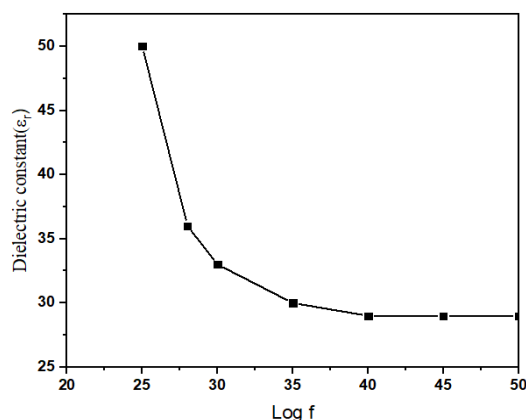


Fig. 10. Dielectric constant Vs Log f for BLSOD.

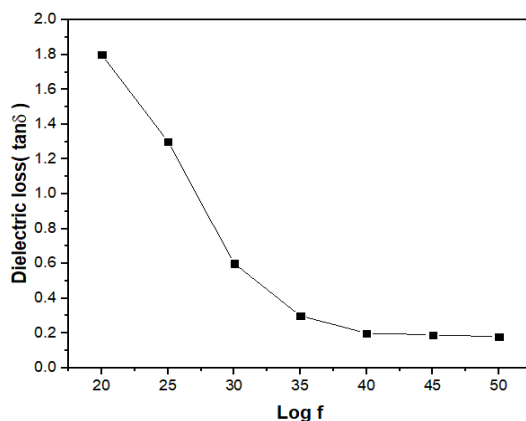


Fig. 11. Dielectric loss Vs Log f for BLSOD.

3.8. NLO Study

The efficiency of second order nonlinear optical (NLO) properties is evaluated using a second harmonic generation (SHG) study on a sample. When good quality single crystals could not be harvested, the Kurtz and Perry powder technique was introduced to study the NLO efficiency of the single crystal in the form of powder [38]. The Kurtz and Perry powder method is a gold standard for evaluating new nonlinear optical materials in development [39]. The widely used technique for confirming the second-order NLO behaviour of a material is the Kurtz-Perry powder technique [40] with KDP crystal as a reference. The BLSOD sample was illuminated with a laser input pulse of 1.9 mJ/p. The SHG in the BLSOD crystal was confirmed by the emission of radiation (532 nm), which proves that the BLSOD single crystal is an NLO material. The efficiency of SHG in BSLOD is found to be 1.1 times that of the standard KDP.

4. Conclusions

The single crystals of Bis-L-Serinium oxalate dihydrate (BLSOD) were grown by the slow evaporation solution growth technique. The grown crystals were characterized by single crystal XRD analysis, and it was found that the structure of the BLSOD crystal belonged to a monoclinic system. FTIR spectral analysis confirmed the presence of functional groups in BLSOD. The UV-

Vis-NIR spectrum confirmed that the crystal is transparent throughout the visible spectrum. The calculated hardness number validates this material for device fabrication. The thermal behaviour of the grown crystal was estimated by the TG/DTA technique. It is evident that the material is thermally stable up to 183°C. Crystals with low dielectric constants have lower losses because they have fewer dipoles per unit volume, and thus BLSOD crystals may be more useful for high-speed electro-optic modulations. The emission of SHG from BLSOD crystal was confirmed by the Kurtz-Perry powder method. The above experimental results clearly show that the grown sample Bis-L-Serinium oxalate dihydrate (BLSOD) crystal can be used as a potential material for NLO applications.

Acknowledgments

The authors are grateful to Dr. M. Vanjinathan, Assistant Professor in Chemistry, D.G.Vaishnav College, Chennai, India for his help and support in the spectral interpretations.

References

- [1] M. Nageshwari, C. RathikaThayaKumari, G. Vinitha, S. Muthu, M. Lydia Caroline, *Physica B: Condensed Matter*, 541(1), 32(2018); <https://doi.org/10.1016/j.physb.2018.04.020>
- [2] P. Geetha, S. Krishnan, R.K. Natarajan, V. Chithambaram, *Current Applied Physics*, 15(3), 201 (2015); <https://doi.org/10.1016/j.cap.2014.11.014>
- [3] Kang Min Ok, Eun Ok Chia, P. Shiv Halasyamani, *Chem.Soc.Rev.* 35(1), 710 (2006); <https://doi.org/10.1039/b511119f>
- [4] Donald M. Burland, Robert D. Miller, Cecilia A. Walsh, D.M. Burland, *Chem. Rev.* 94(1), 31 (1994); <https://doi.org/10.1021/cr00025a002>
- [5] Peng Yu, Li-Ming Wu, Liu-Jiang Zhou, Ling Chen, *J. Am. Chem. Soc.* 136(1), 480 (2014); <https://doi.org/10.1021/ja411272y>
- [6] P. Ramasamy and P. SanthanaRaghavan, "Crystal Growth Processes and Methods," KRU Publications, Kumbakonam, India, 1999.
- [7] G. Madhurambal, P. AnbuSrinivasan, *Cryst. Res. Technol.* 41(3), 231 (2006); <https://doi.org/10.1002/crat.200510565>
- [8] V. Chithambaram, T.S.F. Rajesh, G. Palani, et al.. *J. Opt* 49(2), 181 (2020); <https://doi.org/10.1007/s12596-020-00605-7>
- [9] T. Henningsen, N.B. Singh, R.H. Hopkins, R. Mazelsky, F.K. Hopkins, D.O.Frazier, O.P. Singh, *Materials Letters*, 20(3), 203(1994); [https://doi.org/10.1016/0167-577X\(94\)90088-4](https://doi.org/10.1016/0167-577X(94)90088-4)
- [10] C. C. Frazier, M. P. Cockerham, E. A. Chauchard, and Chi H. Lee, *J.Opt.Soc.Am.B.* 4(1), 1899 (1987); <https://doi.org/10.1364/JOSAB.4.001899>
- [11] M.K.Marchewka, S.debrus, H.Ratajczak, *Cryst.Growth Des.*3(4), 587 (2003); <https://doi.org/10.1021/cg030008v>
- [12] N. Saravanan, V. Ravisankar, & V. Chithambaram, *J Mater Sci: Mater Electron* 29(1), 5009 (2018); <https://doi.org/10.1007/s10854-017-8462-5>
- [13] C. Sindhusa, M. Padma, B. Gunasekaran, H. Marshan Robert, *Journal of Molecular Structure*,doi:10.1016/j.molstruc.127981 (2020).
- [14] R.Raja, R.Sugaraj Samuel, V. Chithambaram, G. Viju, S. Janarthanan,& A. Mohamed Hidayathullah, *Journal of Materials Science: Materials in Electronics*,33(7), 20035 (2022); <https://doi.org/10.1007/s10854-022-08821-6>
- [15] X.Liu, Z. Wang, Z. Zhang, X. Wang, A. Duan, Z. Sun, L. Zhu, D. Xu, *J. Cryst. Growth.*308(1), 130 (2007); <https://doi.org/10.1016/j.jcrysgro.2007.07.051>
- [16] S.Varadarajan, M.S. Kumar, S. Shanmugan, et al. *J Mater Sci: Mater Electron* 32(1) 26351 (2021); <https://doi.org/10.1007/s10854-021-06987-z>

- [17] H.L. Bhat, Bull. Mater.Sci. 17(7), 1233 (1994); <https://doi.org/10.1007/BF02747223>
- [18] Marta Kulik, Aleksandra Pazio and Krzysztof Wozniak, ActaCryst. E69, 1667 (2013).
- [19] K. Boopathi, P. Ramasamy, G. Bhagavannarayana, Journal of crystal growth 386(1), 32 (2014); <https://doi.org/10.1016/j.jcrysgro.2013.09.028>
- [20] A. Fadlelmoula, D. Pinho, V.H, Carvalho, S.O. Catarino, G. Minas, Micromachines (Basel), 13(2), 187 (2022); <https://doi.org/10.3390/mi13020187>
- [21] J. Chai, K. Zhang, Y. Xue, W. Liu, T. Chen, Y. Lu, G. Zhao, Review of MEMS Based Fourier Transform Spectrometers, Micromachines, 11(2), 214 (2020); <https://doi.org/10.3390/mi11020214>
- [22] L.I. Fockaert, T. Würger, R. Unbehau, B. Boelen, R.H. Meißner, S.V. Lamaka, M.L. Zheludkevich, H. Terryn, J.M.C. Mol, ElectrochimicaActa, 345(1) 136166 (2020); <https://doi.org/10.1016/j.electacta.2020.136166>
- [23] R. SathishKumar, G. Arthanareeswaran, A.F. Ismail, M.S. Abdullah, N.B. Cheer, Membrane Characterization, 24(1) (2017), 69-80; <https://doi.org/10.1016/B978-0-444-63776-5.00004-8>
- [24] S H Moolenaar , U F H Engelke, R A Wevers, Ann ClinBiochem. 40(1), 16 (2003); <https://doi.org/10.1258/000456303321016132>
- [25] Sharma, B.K. Goel Publishing House, Krishna Prakashan Media Ltd., Meerut, 193 (2005).
- [26] PalanisamySaritha, SeshathriBharathan, GanesanSivakumar; IOSR- JAP, 4(4), 38 (2013).
- [27] B. Jalel, N. Ennaceur, S. Hawech, R. Henchiri, W. Bouguerra, I. Ledoux-Rak, Journal of Physics and Chemistry of Solids, 133(1), 25 (2019); <https://doi.org/10.1016/j.jpics.2019.04.036>
- [28] N. Sudha , R. Mathammal , R. Shankar , G. Sharon Benita, Optics & Laser Technology. 137(1), 106800 (2021); <https://doi.org/10.1016/j.optlastec.2020.106800>
- [29] K.Naseema, SarathRavi, RakhiSreedharan, Chinese Journal of Physics, 60(1), 612 (2019); <https://doi.org/10.1016/j.cjph.2019.05.037>
- [30] M. Nageshwari , C. RathikaThayaKumari , P. Sangeetha , G. Vinita , M. Lydia Caroline, Chinese Journal of Physics, 56(2) 502 (2018); <https://doi.org/10.1016/j.cjph.2018.02.003>
- [31] A. Cyrac Peter, M. Vimalan, P. Sagayaraj, J. Madhavan, Physica B: Condensed Matter, 405(1), 65 (2010); <https://doi.org/10.1016/j.physb.2009.08.035>
- [32] S. Mary Linet, S. Dinakaran, S. Jerome Das, Journal of Alloys and Compounds, 509(9), 3832 (2011); <https://doi.org/10.1016/j.jallcom.2010.12.083>
- [33] S. Sasi, G. Ramesh, R. Robert, S. Arumugam, C. Inmozhi, Optik. 127(2), 759 (2016); <https://doi.org/10.1016/j.ijleo.2015.10.086>
- [34] Ramesh Tangirala, AnooshaBorra, BankupalliSatyavathi, Prathap Kumar Thella, K. V. Padmaja, Madapusi P. Srinivasan, RajarathinamParthasarathy& Suresh Bhargava, J. Thermal. Anal. Calroi. 147(12), 6807 (2022); <https://doi.org/10.1007/s10973-021-10951-8>
- [35] W. Xiaojun, W. Na, Y. Yanpeng, J. GuoLiang, L. Zhouting, W. Xia, L. Zhiyan, Journal of Energetic Materials, 39(1), 113 (2020); <https://doi.org/10.1080/07370652.2020.1762801>
- [36] G.S. Aswathy, K.C. Bright, Optical Materials, 124(1), 112048 (2022); <https://doi.org/10.1016/j.optmat.2022.112048>
- [37] V.D. Maske, N.S. Meshram, K.G. Rewatkar, Materials Today: Proceedings, 4(11), 11984 (2017); <https://doi.org/10.1016/j.matpr.2017.09.120>
- [38] D. N. Nikogosyan, Nonlinear Optical Crystals: A Complete Survey (Springer, New York, (2005).
- [39] Accurate determination of second order nonlinear optical coefficients from powder crystal monolayers, J. Appl. Phys. 109(1), 113105 (2011); <https://doi.org/10.1063/1.3592964>
- [40] S.K. Kurtz, T.T. Perry, A Powder Technique for the Evaluation of Nonlinear Optical Materials; J. Appl. Phys. 39, 3798 (1968); <https://doi.org/10.1063/1.1656857>